J Mater Sci (2009) 44:3192–3197
DOI 10.1007/s10853-009-3425-8

The influence of thermal annealing on the morphology and structural properties of a conjugated polymer in blends with an organic acceptor material

David E. Motaung · Gerald F. Malgas · Christopher J. Arendse · Sipho E. Mavundla · Clive J. Oliphant · Dirk Knoesen

Received: 5 March 2009 / Accepted: 17 March 2009 / Published online: 31 March 2009

Abstract In this report, the influence of thermal annealing of thin P3HT films and P3HT:C_{60} composites were studied regarding their morphology and structural properties. Atomic force microscope measurements on P3HT films and P3HT:C_{60} composite disclose some variation in morphology during annealing due to the crystallization of C_{60}. The as-prepared P3HT:C_{60} films have a higher surface roughness and larger cluster size compared to the as-prepared P3HT films. The thermal annealing effects on the optical microscopy indicate that the polymer shows improved capability to self-organize. Their structural properties were studied by X-ray diffraction analysis. It was found that the crystallinity of the investigated films is drastically increased upon annealing and a decrease in the grain sizes is observed.

Introduction

Plastic solar cells consisting of an interpenetrating network of fullerenes and conjugated polymers have gained wide spread scientific interest during the last decade due to their low production cost and easy solution processing, low specific weight mechanically flexibility [1–3]. Currently, the best devices consist of a single bulk-heterojunction (BHJ) active layer, where the polymer (donor) and fullerene (acceptor) are deposited from a common solvent. As the solvent dries the donor and acceptor components separate into domains. The eventual efficiency of the solar cell has shown to be extremely sensitive to the size, morphology, composition, and the crystallinity of the formed domains [4, 5].

Enhancement of the morphology in devices fabricated with a mixture of regio-regular poly(3-hexylthiophene) (P3HT) and [6,6]-phenyl C_{61}-butyric acid methyl ester (PCBM) has been observed with the use of heat treatment methods, such as solvent annealing [6] and thermal annealing [3, 7–9] resulting in solar cells with higher power efficiencies (5%). The increase in solar cell efficiency can be explained by simultaneously increasing the optical absorption as well as the charge carrier mobilities, which are correlated to the enhanced crystallization of P3HT during annealing [3]. Aasmundtveit et al. [10] reported that polythiophenes tend to crystallize in pristine P3HT films. Recently, it was shown by electron diffraction that P3HT is also capable of a crystalline organization in blends with methanofullerenes [11].

Recently, power conversion efficiencies of up to 6.5% were reached for polymer tandem cells [12]. This progress has put polymer solar cells one step closer to commercialization. In this article, the influence of thermal annealing on the morphology and structural changes of P3HT were investigated. The morphological changes of the active layers were monitored using various techniques. The *d*-spacing and size of polymer crystallites of as-prepared and annealed P3HT and its blends films were determined.

D. E. Motaung · G. F. Malgas (✉) · S. E. Mavundla · C. J. Oliphant
National Centre for Nano-structured Materials, Council for Scientific Industrial Research, P.O. Box 395, Pretoria 0001, South Africa
e-mail: gmalgas@csir.co.za

D. E. Motaung · C. J. Arendse · D. Knoesen
Department of Physics, University of the Western Cape, Private Bag X17, Bellville 7535, South Africa

S. E. Mavundla
Department of Chemistry, University of the Western Cape, Private Bag X17, Bellville 7535, South Africa

The combination of XRD and atomic force microscopy (AFM) exhibited the difference between crystallization and the morphology of P3HT and C_{60} during the annealing process.

Experiment details

Sample preparation

All the chemicals used in this experiment were purchased from Sigma Aldrich. rr-P3HT was used as a light absorption and electron donating material; while fullerene (C_{60}) was used as an electron acceptor material. The molecular weight (M_n) of P3HT reported by Sigma Aldrich was ~64,000; with regularity that is greater than 98.5% for head-to-tail. These materials were used as received, without any further purification. Indium tin oxide (ITO) coated on a 1-mm glass substrate with a resistance between 8 and 12 Ω/square, and silicon (Si) substrates were successfully cleaned with acetone and isopropyl alcohol and dried in dry nitrogen. A mixture of rr-P3HT (5 mg) and C_{60} (5 mg) was dissolved in 1 mL of chloroform solution. The solution was stirred over night at a temperature of 50 °C to maximize mixing of P3HT:C_{60} solution. The solubility of C_{60} fullerene on a chloroform solution was reported to be about 0.16 mg/mL [13]. P3HT and its blends with a thickness of about 100 nm were spin coated onto the Si substrates. The samples were dried on a hot plate at a temperature of 50 °C for 15 min.

Characterization

A Tecnai F20 field emission high-resolution transmission electron microscope (HR-TEM), operated at 120 kV was employed to examine the internal structure and crystallinity of rr P3HT. Specimens for HR-TEM analysis were prepared by dispersing the P3HT in chloroform, of which a drop was subsequently transferred to a holey-carbon copper grid and dried at ambient conditions. AFM images of the top surface of thin films of rr P3HT and its blends spin coated on Si (110) substrates in a tapping mode were analyzed using a Veeco AFM system (Digital Instruments) at ambient conditions. A Polarised Optical Microscope (Carl Zeiss axiovisson) with a magnification of 100× was employed to study the optical morphology of the as-prepared P3HT films with that annealed at different temperatures for 30 min. Film thickness was measured using a Veeco DEKTAK 6M Stylus profilometer.

A Philips PW 1830 X-ray diffractometer with a Cu Kα ($\lambda = 0.154$ nm) monochromated radiation source, operating at 45.0 kV and 40.0 mA was utilized in order to determine the crystallinity of P3HT film and its blends spin coated onto a Si substrate. XRD data were collected in the 2θ ranging from 3° to 40° with a step size of 0.02°. The grain sizes of the films were calculated using the Scherer formula.

Results and discussion

Atomic force microscopy measurements

The morphology of the polymer/acceptor composite or photoactive layers, that play a key role in the final solar cell performance, can be strongly modified and improved by thermal annealing. The surface topography obtained from an AFM usually gives a good insight into the film formation ability and the tendency of the components to phase separate. Figure 1 shows a series of AFM images of the P3HT and its blends obtained in tapping mode. The surface of the as-prepared P3HT on a Si substrate and P3HT:C_{60} (1:1 wt%) films is very smooth with a root mean square (rms) roughness (σ_{rms}) of 1.375 and 1.679 nm, respectively. The film does not show any coarse separation into different phases. The P3HT:C_{60} (1:1 wt%) film (Fig. 1d) shows a higher surface roughness, which is probably due to the addition of the fullerene (C_{60}) forming clusters around the film.

However, upon annealing at 110 °C for 30 min (Fig. 1b), the surface roughness of P3HT increases up to 7.89 nm, while P3HT:C_{60} (1:1 wt%) film (Fig. 1e) shows a pronounced surface roughness of about 18.90 nm. When the samples were annealed at 150 °C, the surface roughness increased up to 8.25 and 19.31 nm for P3HT and the blend, respectively. It is evident in Fig. 1 that the annealed samples show a much coarser texture with broad "hill-like" features compared with the as-prepared samples. The rough surface is probably a signature of polymer reorganization, which in turn enhances ordered structure formation in the thin film and also increases the carrier mobility, which could produce a higher efficiency from the devices. This suggests that there is a thermodynamic driving force for the sample to reorganize toward a more stable equilibrium and thus to phase separate. However, excessive roughness makes phase segregation excessively comparable to the exciton diffusion length, which leads to the reduced charge segregation and device efficiencies. Similar results were also observed in the literature [14–16]. Recent morphological and structural studies [11] have shown that in P3HT:PCBM active layers, the crystallization and the demixing are interdependent parameters.

Transmission electron microscopy measurements

The HR-TEM micrograph presented in Fig. 2 illustrates that the rr-P3HT are crystalline. The micrograph shows a

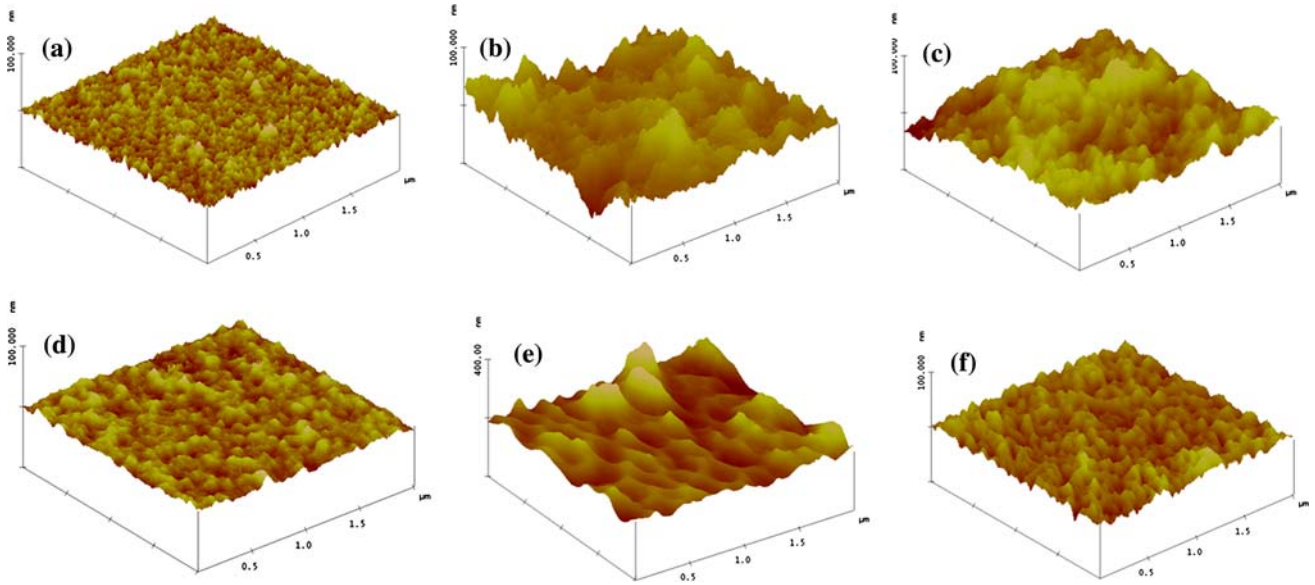

Fig. 1 AFM height images (2 μm × 2 μm size) of the surface of the active layer consisting of **a** as-prepared pure P3HT, **b** annealed at 110 °C, **c** annealed at 150 °C, **d** as-prepared P3HT:C_{60} (1:1 wt%), **e** P3HT:C_{60} (1:1 wt%) annealed at 110 °C, and **f** annealed at 150 °C. Note all the samples were annealed for 30 min

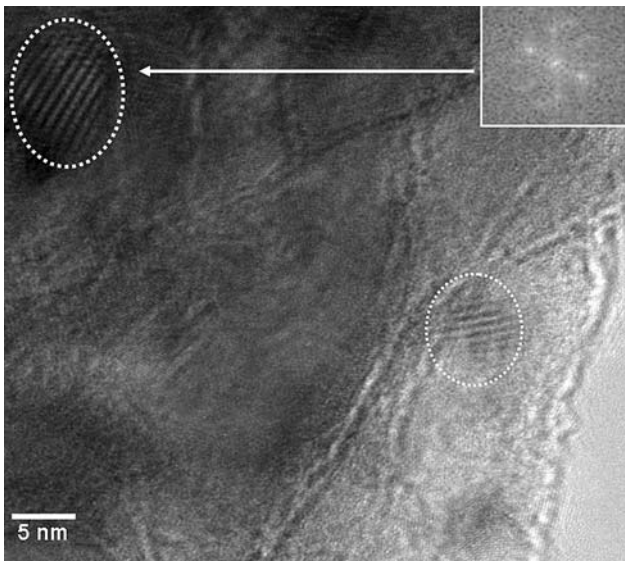

Fig. 2 HR-TEM micrograph of the rr-P3HT film and the corresponding fast Fourier transform (FFT) of the selected area (inset)

homogeneous layer without any obvious phase separation. The inset in Fig. 2 corresponds to the fast Fourier transform (FFT) of the selected area. The FFT shows a very low crystallinity of P3HT indicating that P3HT material is composed of an amorphous polymer matrix with crystalline regions (circled in Fig. 2), which possess a spacing of $\sim 0.8 \pm 0.06$ nm, corresponding to the (200) planes. Drees et al. [17] also reported a bright field TEM image of P3HT showing a large and extended disordered (amorphous) zone between the crystalline lamellae.

Optical microscopy measurements

Bright field optical microscopy micrographs of as-prepared P3HT films and P3HT:C_{60} (1:1 wt%) blends compared with that annealed at 110 and 150 °C for 30 min are shown in Fig. 3. It is evident in Fig. 3a that the as-prepared P3HT film is relatively smooth with tarnishes (small stains). When these films are annealed their optical contrast changes, the film becomes rougher and agglomerations of the films are observed. These changes in the optical micrographs are due to the annealing, indicating an enhancement in the crystallinity of the P3HT films.

Moreover, when P3HT sample was blended with a C_{60} fullerene, P3HT:C_{60} (1:1 wt%) (Fig. 3d), the as-prepared blend film showed an irregular behavior and with larger agglomeration (spheres) as compared to as-prepared and annealed P3HT film. These agglomerations (or spheres) are related to C_{60}. However, when the blend is annealed, the spheres become bigger and show an increase in coarseness. The clustering of the spheres is probably due to a diffusion of C_{60} into P3HT during annealing. This is in good agreement with results obtained by the AFM technique as well the results reported by Nguyen et al. [18]. Campoy-Quiles et al. [19] observed color visible changes during a continuous heating cycle of P3HT. They also showed that these visible color changes may correspond to P3HT crystallization, which is then followed by melting of the material.

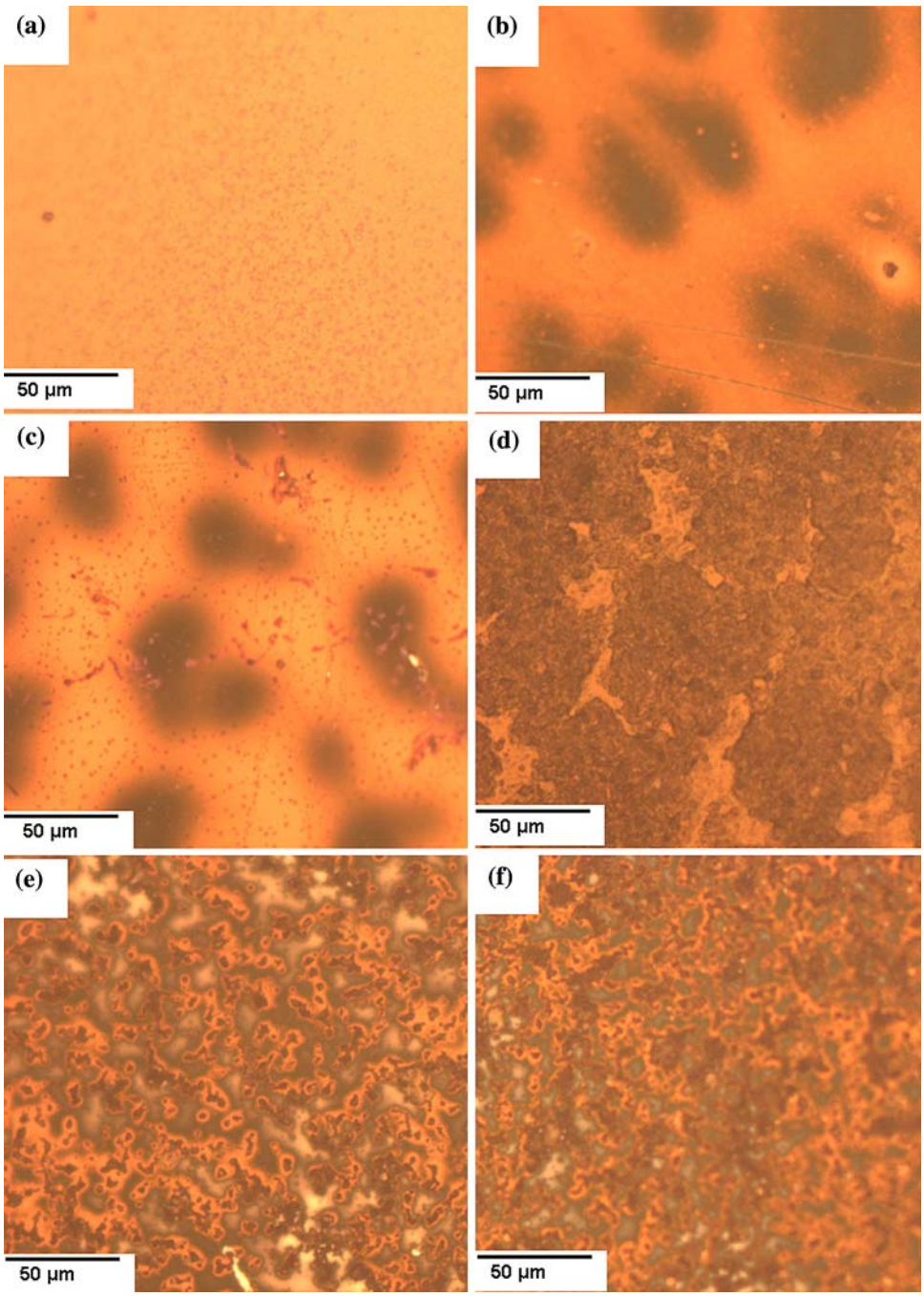

Fig. 3 Optical microscopy images of **a** as-prepared P3HT, **b** P3HT film annealed at 110 °C, **c** P3HT film annealed at 150 °C, **d** as-prepared P3HT:C_{60} (1:1 wt%) blend, **e** annealed blend at 110 °C, and **f** annealed blend at 150 °C. Note all the samples were annealed for 30 min

X-ray diffraction measurements

For a detailed study of the structural ordering of rr-P3HT, an XRD diffraction technique was used. Additionally, the changes upon thermal annealing of the films for 30 min at different temperatures were analyzed. Figure 4 shows the XRD spectra of the as-prepared P3HT films and it blends P3HT:C_{60} (1:1 wt%) compared with that annealed at 110 and 150 °C for 30 min, respectively. The as-prepared sample shows a single diffraction peak before annealing at $2\theta = 5.4°$, which is associated with the lamella structure of thiophene rings in P3HT [20]. Upon annealing, the sample shows a secondary peak (200) at 10.8° and tertiary peak (300) at 15.9° indicating that all pristine P3HT films show a well-organized intraplane structure. The diffraction patterns of Fig. 4 correspond to as described by the JCPDS {48-2040}. The peak indicated by the arrow at about 28. 1° is associated with the Si substrate. However, the blend in Fig. 4b showed (220), (311), (222), and (331) diffraction peaks at 17.7, 20.9, 21.7, and 27.4° , respectively, upon

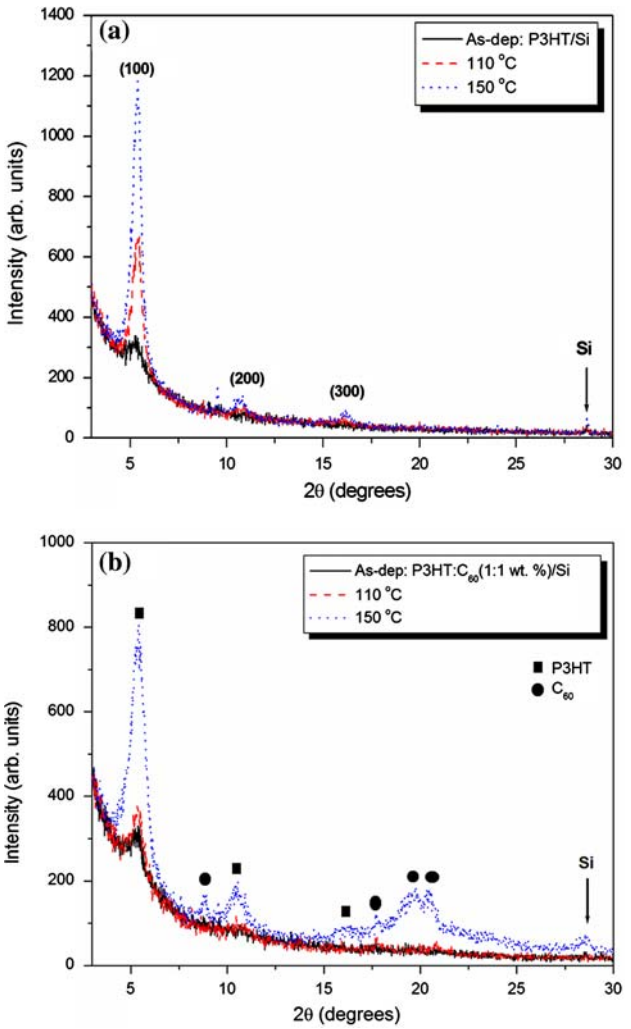

Fig. 4 XRD patterns of as-prepared and annealed **a** rr-P3HT film and its blend, **b** P3HT:C_{60} (1:1 wt%) at 110 and 150 °C for 30 min. The P3HT peaks are indicated by a *square* and C_{60} by a *circle*

annealing at 150 °C, which are associated with a C_{60} fullerene as described by the JCPDS {47-0787, 44-0558}. The corresponding lattice constant *d,* can be calculated using Bragg's law:

$$2d\sin(\theta) = n\lambda \quad (1)$$

where $\lambda = 0.154$ nm is the wavelength of incident beam, 2θ the angle between incident and scattered X-ray wave vectors, and n the interference order.

Therefore, using Eq. 1, we obtain $d = 1.64 \pm 0.05$ nm, 0.82 ± 0.05 nm, and 0.56 ± 0.05 nm. The 0.82 nm spacing is similar to the *d*-spacing found in the TEM results. The detected peak originates from the P3HT crystallites with *a*-axis orientation (polymer backbone parallel and side chains perpendicular to the substrate) [21]. However, no diffraction peaks corresponding to the P3HT crystallites with other orientations such as polymer backbone and side chains parallel to the substrate were observed [22]. The mean sizes of the P3HT crystallites at (100) reflection L_{100} can be obtained using Scherrer's relation [23, 24]:

$$L = \frac{0.9\lambda}{B_{2\theta}\cos(\theta)} \quad (2)$$

where λ is the wavelength of the X-rays, $B_{2\theta}$ the full width at half maximum intensity FWHM), and θ the diffraction angle. Therefore, employing Scherer formula (2), we obtain the grain size of P3HT and P3HT:C_{60} films at different annealing temperatures as shown in Table 1.

Table 1 Grain size of P3HT and P3HT:C_{60} (1:1 wt%) films for different annealing temperatures

	P3HT film			P3HT:C_{60} composite film		
Temperature (°C)	RT	110	150	RT	110	150
Grain size (nm)	12.2	13.4	15.9	17.2	14.7	12.1

As shown in Fig. 4 and Table 1, the emergence of a crystalline phase in the as-prepared samples is observed that are in good agreement with the HR-TEM results. This crystalline phase becomes more pronounced at a temperature of 150 °C. A minimum grain size of 12 nm is found in the as-prepared P3HT sample. At around 150 °C, the grain size growth is well increased. This indicates an increase in the ordering of the alkyl chains within the main thiophene chains. However, when a P3HT is blended with C_{60} fullerene (1:1 wt%), the FWHM of P3HT at 5.4° increases with the annealing temperature. The increase in a FWHM (reduction in grain sizes) as well a slight decrease in P3HT crystallites is due to a disordering of P3HT chains caused by an addition of C_{60} fullerene. This can also be due to a diffusion of C_{60} molecules out of the P3HT matrix forming larger clusters leading to a phase separation of P3HT and C_{60}.

Kline et al. [25] reported that films of higher molecular weight P3HT produces a broader XRD peak suggesting a more disordered film with smaller crystalline domains. The authors argue that the smaller π-stacked domains, connected by disordered polymer chains, would enable easier charge transport through the film and prevent charge trapping within crystalline domains or at grain boundaries. Chiu et al. [26] showed that when P3HT is blended with PCBM, the P3HT crystallite size reduces with an increase in annealing temperature and resulted in an increase in the short circuit current density (J_{sc}). They also showed that the particles of PCBM become larger and subsequently lead to better pathways for electron transport. Additionally, the C_{60} clusters also enable better hole transport in the polymer phase. However, Huang et al. [27] demonstrated that longer annealing time (more than 60 min) exhibit too larger PCBM clusters, which leads to decrease in charge transport and device efficiency. It should be noted, that the

obtained values correspond to the domain size along the *a*-axis and that no crystal with *b*- or *c*-axis orientation was detected. Similar results on *d*-spacing were reported by Kim et al. [28] and Erb et al. [22].

Conclusion

In conclusion, we have studied the morphology and structural properties of P3HT films and P3HT:C_{60} composite films both as-prepared and annealed at different temperatures. AFM measurements showed that the blends have a higher surface roughness compared to the pure P3HT films. After annealing, the surface roughness of pure P3HT and P3HT:C_{60} (1:1 wt%) film increased; this can be related to a signature of polymer reorganization, which in turn enhances ordered structure formation in the thin film. HR-TEM results showed a homogeneous layer of P3HT film without any obvious phase separation. The TEM studies also exhibited very low features of crystallization that indicates that it is composed of an amorphous network with crystallites embedded in it. XRD studies have also demonstrated the crystalline nature of pure P3HT films. The as-prepared P3HT-films were found to be partially crystalline, whereas the crystallinity increases as the temperature increases. In the case of the film annealed at 150 °C; a crystallite size of 15.9 nm was obtained from analysis of the X-ray diffraction pattern. A slight decrease in P3HT crystallites and an increase in grain sizes were observed when a P3HT:C_{60} (1:1 wt%) blended structure was prepared. This is due to a disordering of P3HT chains caused by the addition of fullerene. Upon annealing a reduction in the grain sizes was also observed. This is probably due to a diffusion of C_{60} molecules out of P3HT matrix forming larger clusters leading to a phase separation of P3HT and C_{60}.

Aknowledgements The authors would like to thank the financial support of the Department of Science and Technology of South Africa and the Council for Scientific Industrial Research (CSIR), South Africa (Project No. HGERA7S). The authors are especially thankful to Jayita Bandyopadhyay (National Centre for Nano-Structured Materials, CSIR) for her valued assistance with the optical microscopy analysis.

References

1. Sun S-S, Sariciftci NS (2005) Organic photovoltaics: mechanisms, materials, and devices. CRC Press, Boca Raton, FL
2. Brabec CJ, Dyakonov V, Parisi J, Sariciftci NS (2003) Organic photovoltaics: concepts and realization. Springer, Berlin, Germany
3. Ma W, Yang C, Gong X, Lee K, Heeger AJ (2005) Adv Funct Mater 15:1617
4. Hoppe H, Sariciftci NS (2006) J Mater Chem 16:45
5. Halls JJM, Arias AC, MacKenzie JD, Wu WS, Inbasekaran M, Woo EP, Friend RH (2000) Adv Mater 12:498
6. Li G, Yao Y, Yang H, Shrotriya V, Yang G, Yang Y (2007) Adv Funct Mater 17:1636
7. Padinger F, Rittberger RS, Sariciftci NS (2003) Adv Funct Mater 13:85
8. Yang XN, Van Duren JKJ, Rispens MT, Hummelen JC, Janssen RAJ, Michels MAJ, Loos J (2004) Adv Mater 16:802
9. Camaioni N, Ridolfi G, Casalbore-Miceli G, Possamai G, Maggini M (2002) Adv Mater 14:1735
10. Aasmundtveit KE, Samuelsen EJ, Guldstein M, Steinsland C, Flornes O, Fagermo C, Seeberg TM, Pettersson LAA, Inganäs O, Feidenhansl R, Ferrer S (2000) Macromolecules 33:3120
11. Yang X, Loos J, Veenstra SC, Verhees WJH, Wienk MM, Kroon JM, Michels MAJ, Janssen RAJ (2005) Nano Lett 5:579
12. Kim JY, Lee K, Coates NE, Moses D, Nguyen T-Q, Dante M, Heeger AJ (2007) Science 317:222
13. Ruoff RS, Tse DS, Malhotra R, Lorents DC (1993) J Phys Chem 97:3379
14. Li G, Shrotriya V, Yao Y, Yang Y (2005) J Appl Phys 98:043704
15. Kim Y, Choulis SA, Nelson JJ, Bradley DDC (2005) J Mater Sci 40:1371. doi:10.1007/s10853-005-0568-0
16. Yu H-Z, Peng J-B (2008) Chin Phys Lett 25:1411
17. Drees M, Hoppe H, Winder C, Neugebauer H, Sariciftci NS, Schwinger W, Schaffler F, Topf C, Scharber MC, Zhud Z (2005) J Mater Chem 15:5158
18. Nguyen LH, Hoppe H, Erb T, Günes S, Gobsch G, Sariciftci NS (2007) Adv Funct Mater 17:1071
19. Campoy-Quiles M, Ferenczi T, Agostinelli T, Etchegoin PG, Kim Y, Anthopoulos TD, Stavrinou PN, Bradley DDC, Nelson J (2008) Nature Mater 7:158
20. Kim JY, Kim SH, Lee HH, Lee K, Ma W, Gong X, Heeger AJ (2006) Adv Mater 18:572
21. Erb T, Raleva S, Zhokhavets U, Gobsch G, Stuhn B, Spode M, Ambacher O (2004) Thin Solid Films 450:97
22. Erb T, Zhokhavets U, Hoppe H, Gobsch G, Al-Ibrahim M, Ambacher O (2006) Thin Solid Films 511:483
23. Warren BE (1990) X-ray diffraction. Dover, New York, p 251
24. Cullity D (1956) Elements of X-ray diffraction. Addison-Wesley, Reading, MA
25. Kline RJ, McGehee MD, Kadnikova EN, Liu J, Frechet JMJ (2003) Adv Mater 15:1519
26. Chiu M-Y, Jeng U-S, Su C-H, Liang KS, Wei KH (2008) Adv Mater 20:2573
27. Huang Y-C et al (2008) Sol Energy Mater Sol Cells. doi:10.1016/j.solmat.2008.10.027
28. Kim Y, Cook S, Tuladhar SM, Choulis SA (2006) Nature Mater 5:197